Vorticity dynamics and control of self-propelled swimming of a 3D ray

Chuijie WU[1,*], Zhiqiang XIN[2]

[1]Schoole of Aeronautics and Astronautics, Dalian University of Technology, Dalian, CHINA
[2]College of Mechanics and Materials, Hohai University, Nanjing, CHINA
*corresponding author: cjwudut@dlut.edu.cn

Abstract The self-propelled swimming of a 3D ray is investigated by combining the control strategy of fish swimming and unsteady computational fluid dynamics numerical algorithm with moving boundary in this study. The 3D computational fluid dynamics software package contains the immersed boundary method, volume of fluid method and the adaptive multi-grid finite volume method. Through the flow control of the 3D traveling wave, the three-dimensional large-scale vortex structures in the wake of an undulation ray are eliminated, and the fluid mechanisms of self-propelled swimming of a 3D undulation ray are analyzed in depth. The impacts of the waveform, wave frequency, wavelength and amplitude of the 3D traveling wave on the force applied on body and wake structure are also studied.

Keywords: adaptive multi-grids, immersed boundary method, traveling wave, self-propelled swimming, eliminate wake vortices

1 Introduction

In nature, fish/insects are capable of controlling flow using active or passive deformation of body surface, and have more excellent movement performance than man-made vehicles. Many studies have shown that the traveling wave motion can reduce drag force and suppress turbulence as a credible method of turbulent flow control (Wu, Wang and Wu, 2007). So far no theory is available to predict the optimal parameters of the flow control for the traveling wave movement. The fluid mechanisms of the three-dimensional traveling wave are especially unknown. An undulatory ray is propelled by the enlarged pectoral fin on both sides of body, which are undulating in the form of a three-dimensional traveling wave (Blevins and Lauder, 2012). The numerical simulation of the self-propelled swimming of a three dimensional bionic ray are carried out in this study.

2. Computational fluid dynamics numerical algorithm with moving boundary

The finite volume method is used to solve incompressible unsteady Navier-Stokes equations in the present study. The computational domains are spatially discretized using cubic finite volumes organized hierarchically as an octree. The Poisson equation of pressure is solved using the projection and the multi-levels methods. The second order Godunov type scheme is used to discretize the convective terms. The diffusion terms are discretized with the implicit Crank-Nicolson scheme that can eliminate the viscous stability constraint. The temporal discretization is performed using the fractional-step projection method.
The study of fish self-propelled swimming is a moving boundaries problem involving complex geometry. The computing methods of moving boundaries problem are usually classified into the body-fitted moving mesh method and immersed boundary method(IBM) for computational fluid dynamics. In this study, moving boundaries are treated with ghost-cell IBM, which employ discrete forcing where the forcing is either implicitly or explicitly applied to the discretized Navier-Stokes equations. The technique of adaptive multi-grids is used and the adaptive refinement criteria are both vorticity and ∇T, where T is a tracer of VOF. This ensures that meshes intersecting with moving body boundaries are the finest and the accurate representation of moving boundaries is achieved. The detail of numerical algorithms is referred to Xin and Wu(2012).

3. Motion equations and undulation parameters of a 3D undulation ray

The dynamics equations for the self-propelled 3D undulation ray are

$$m\frac{d\boldsymbol{u}}{dt} = \boldsymbol{F} \quad , \quad m\frac{d\boldsymbol{L}}{dt} = \boldsymbol{M} \tag{1}$$

$$\boldsymbol{F} = -\int_{\partial B}\left(-p\boldsymbol{n} + \mu\omega \times \boldsymbol{n}\right)dS \tag{2}$$

$$\boldsymbol{F} = -\int_{\partial B}\rho\boldsymbol{x} \times \left(\tfrac{1}{2}\boldsymbol{\gamma}_p + \boldsymbol{\gamma}_{vis}\right)dS \tag{3}$$

where m is the mass of the fish; $\boldsymbol{u}$ is the velocity vector; $\boldsymbol{F}$ is the hydrodynamic force; $\boldsymbol{M}$ is the moment and $\boldsymbol{L}$ is the moment of momentum. Equation (2) is a force formula derived directly from the momentum balance, and equation (3) is a force expression of the boundary vorticity flux. $\partial\boldsymbol{B}$ is 3D fish body surface, $\boldsymbol{n}$ is the unit outer-pointing normal vector of body surface, ρ, μ, $\boldsymbol{\omega}$ are fluid density, dynamic viscosity and vorticity, respectively.

$\boldsymbol{\gamma}_p = \boldsymbol{n} \times \nabla p/\rho$, $\boldsymbol{\gamma}_{vis} = \upsilon(\boldsymbol{n} \times \nabla) \times \boldsymbol{\tau}$ are the boundary vorticity flux caused by the tangential pressure gradient and a viscous vortical effect, respectively(Wu et al., 2006). In the study of self-propelled process of 3D undulation ray, two sets of coordinates are used, which are the fish body coordinates(x_l, y_l , z_l) and the global coordinates(x, y, z). Two sets of coordinates can be converted.

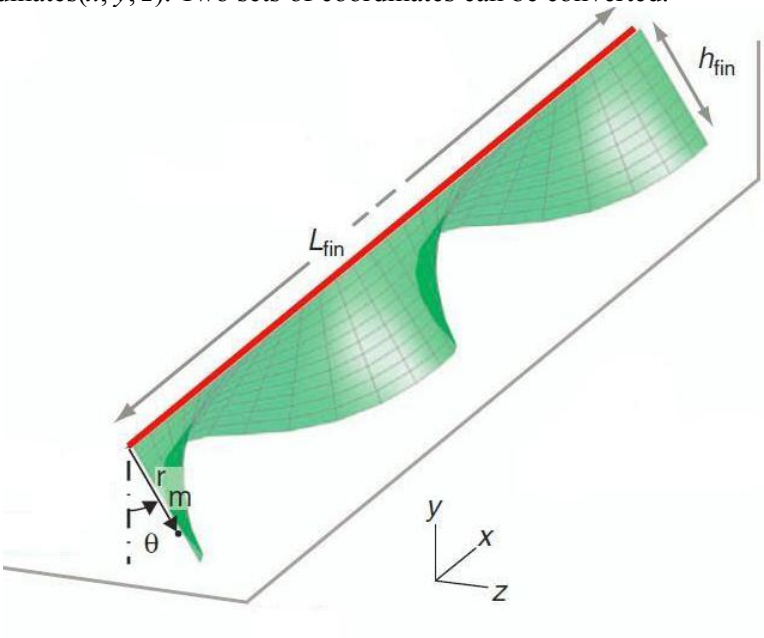

Fig. 1. Schematic diagram of the 3D traveling wave of pectoral fins of an undulation ray

Figure 1 is a schematic diagram of the 3D traveling wave of pectoral fins of an undulation ray. The angular position $\theta(x,t)$ of any point on the pectoral fins is defined by

$$\theta(x,t) = \theta_{\max}\sin 2\pi\left(\frac{x}{\lambda} - ft\right), \tag{4}$$

Where $\theta_{\max}$ is the maximum angular amplitude of the fin from the (x-y) plane, λ is the wavelength, f is frequency, x is the coordinate in the vertebral line direction and t is time. Correspondingly, differentiation of Eqn4 with respect to time yields the velocity $\boldsymbol{u}_{\text{fin}}$ of any point on the pectoral fin (Shirgaonkar et al., 2008). It is defined by

$$\mathbf{u}_{fin} = r_m\frac{\partial\theta}{\partial t}(\sin\theta\mathbf{j} + \cos\theta\mathbf{k}), \tag{5}$$

where $r_m = |\mathbf{r}_m|$ is the distance of a point on the fin from the vertebral line, $\boldsymbol{j}$ and $\boldsymbol{k}$ are unit vectors in the y and z directions, respectively. From undulation rules of the 3D ray, the velocity on the body boundary is obtained, which consists of velocity arising from hydrodynamic force, linear velocity arising from rotation and velocity arising from flapping.

4. Results and analysis

In this study, the computational region is like a flume without inflow and outflow. The dimensionless body length of the 3D ray is 0.6. The attended pectoral fin of an undulatory ray can form a backward or forward propagation traveling wave in the process of self-propelled swimming. The excellent swimming controls are achieved by adjusting wavelength, frequency and the direction of wave propagation. The analyses focus on the fluid mechanic mechanisms to eliminate wake vortex of a 3D self-propelled swimming ray in the following section. The λ_2 method of Jeong and Hussain(1995) was applied to illustrate the 3D vortical structure. From Figure 3, the undulation ray with the initial shape produces one pair of hairpin vortex, while the variations of amplitudes of the center line of the 3D ray in the（y-z） plane is as shown in Figure 2(a). The wake vortices cannot be eliminated completely. This is mainly because the no deformation part in the middle regions of the body surface resulted in the generation of high boundary vorticity flux, thus large-scale vortex structures are created and shed from ray body.

(a) initial (b) amendment

Fig. 2. Variations of amplitudes of the center line of the 3D ray in the（y-z）slice plane

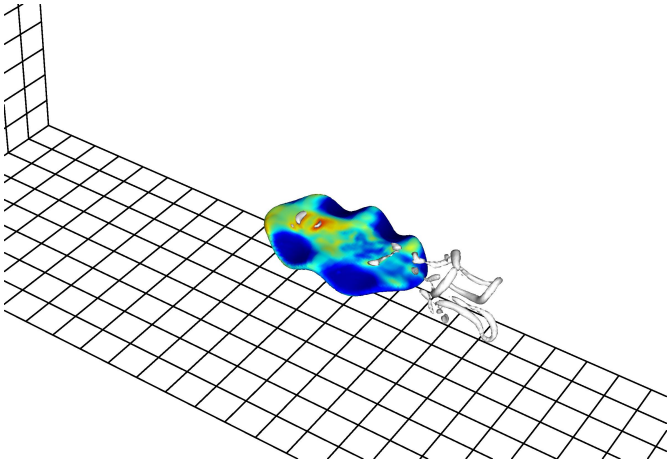

Fig. 3. 3D vortex structures of the undulation ray with the initial shape

In order to eliminate the wake vortices, the area of the regions that does not fluctuate is reduced, and the center line of the 3D ray in the（y-z）slice plane adopts smooth curves, as showing in Figure 2(b). Figure 4 (a) plots the 3D vortical structures of self-propelled swimming of an undulatory ray shown in the isosurfaces of λ_2, and the color on the surface of ray body shows the vorticity distribution. The fish swims in the negative x direction, as shown in Figure 4 (a). It can be seen from Figure 4 (a) that the large-scale vortex does not exist in in the swimming wake of a ray. Thus the vortical wake of a wavy ray is eliminated. From the vorticity distribution of ray body surface, the vorticity only generates at the crest of traveling wave and in middle vertebral part of ray body. From Figure 4 (b), it can be seen that the ray body is wrapped in the regions with relatively high vorticity, and no vortices are shed in to the downstream of 3D ray. The 3D undulatory ray makes good use of vortices. Thus, the swimming efficiency of a undulatory ray is higher. Figure 4 (c) shows the pressure distribution of self-propelled swimming of an undulatory ray. The low pressure region and high pressure region occur on the forward and backward face of the wavy wall, respectively as shown in Figure 4 (c). Thus, the thrust on ray body is negative, which direction is forward. Figure 4 (d) a negative pressure regions are generated upstream of the wave crest of the upper and lower surfaces of a ray, and the regions on downstream of the wave crest is positive pressure area. It elucidates

clearly the fluid mechanism of self-propelled swimming of undulatory ray that the favorable thrust is yielded by adjusting the pressure distribution of moving surface.

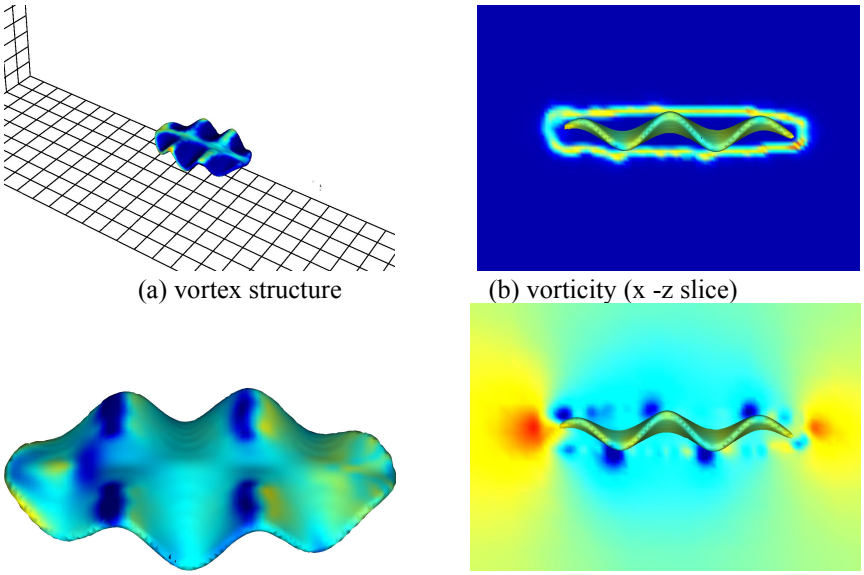

(a) vortex structure (b) vorticity (x -z slice)

(c) pressure on the ray body (d) pressure (x-z slice)

Fig. 4. Fluid fields of self-propelled swimming of a three dimensional bionic ray

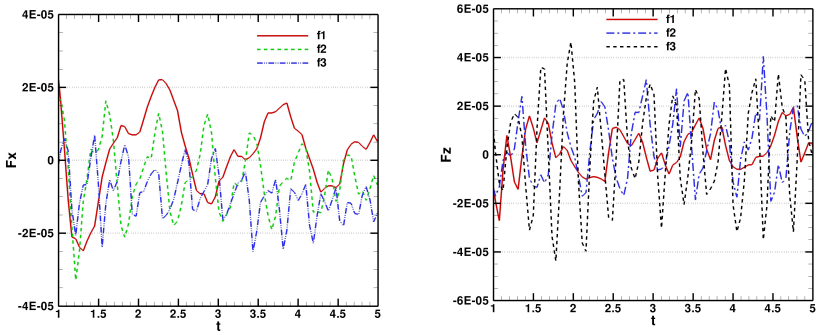

(a) Thrust (b) Heave forces

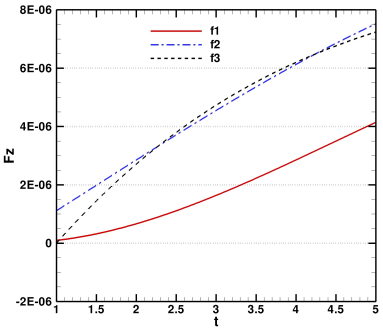

(c) average heave forces

Fig. 5. Thrust and heave forces corresponding to the different frequencies in the process of self-propelled swimming of a 3D bionic ray

Figure 5 presents thrust and heave forces corresponding to the different wave frequencies in the process of self-propelled swimming of a 3D bionic ray. In Figure 5(a) and (b), f_1, f_2 and f_3 denote frequency of the three-dimensional traveling wave $f = 1$, $f = 2$ and $f = 3$, respectively. In these cases, the wavelength is $\lambda = 0.2$, and the maximum angle of wave is $\theta_{max} = 0.25$. The thrust and heave forces shown in Figure 5 (a) and (b) are the instantaneous value. The thrust on ray body usually becomes higher with the increases in frequency, from

Figure 5(a). At the same time, the lift is improved as the frequency increases, but not continues to increases, as shown in Figure 5(b). But it can be seen from Figure 5 (b) that the differences in the lift forces for different wave frequencies are not clear. Therefore, the comparative analyses of the force applied on ray body are carried out using the average force in wave cycle, as shown in Figure 5(c).

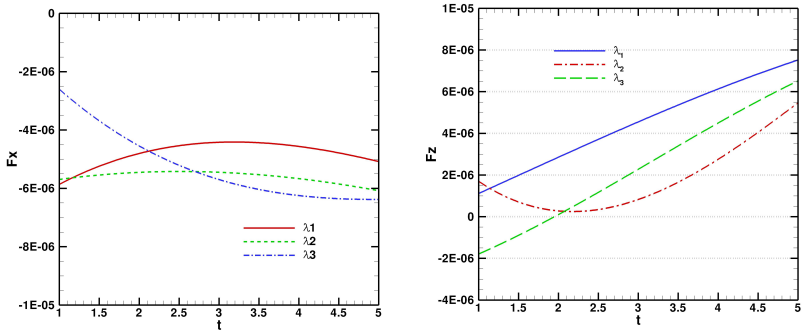

(a) Thrust (b) Heave forces

Fig. 6. Thrust and heave forces corresponding to the different wavelengths in the process of self-propelled swimming of a 3D bionic ray

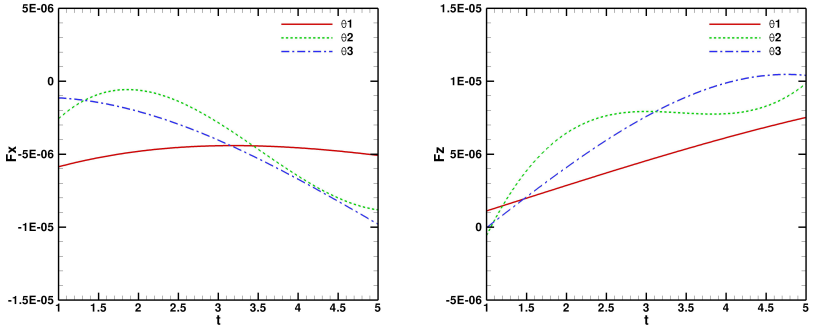

(a)Thrust (b) Heave forces

Fig. 7. Thrust and heave forces corresponding to the different θmax in the process of self-propelled swimming of a 3D bionic ray

Based on the same reasons, the average forces in wave cycle are used to compare the forces corresponding to different wavelengths and amplitudes. In Figure 6(a) and (b), $\lambda 1$, λ_2 and λ_3 mean wavelength $\lambda = 0.2$, $\lambda = 0.3$ and $\lambda = 0.6$, respectively. It can be seen from Figure 6 (a) and (b) that the thrust and heave forces do not varies significantly with wavelength. As the wavelength is too great or small, the thrust are relatively small. In Figure 7(a) and (b), θ_1, θ_2 and θ_3 mean wavelength $\theta_{max} = 0.2$, $\theta_{max} = 0.35$ and $\theta_{max} = 0.45$, respectively. Figure 7 shows that the amplitudes has a small effect on the thrust force, but appropriate amplitude can increase the lift.

5. Conclusion

The 3D large-scale vortex structures of self-propelled swimming of an undulation ray can be eliminated completely with the flow control of 3D traveling wave. While the large-scale wake vortices are eliminated, the vortices only generate at the crest of traveling wave and in middle vertebral part of ray body, and the favorable thrust is yielded by adjusting the pressure distribution of moving surface, which is induced by the vortices. It must choose the combination of optimal wave parameters, in order to achieve excellent swimming performance.

References

[1] Blevins E L, Lauder G V(2012). Rajiform locomotion: three-dimensional kinematics of the pectoral fin

surface during swimming in the freshwater stingray Potamotrygon orbignyi. *J. Exp. Biol.*, 215, pp.3231-3241.
[2] Jeong J, Hussain F(1995). On the identification of a vortex. *J Fluid Mech*, 285, pp.69-94.
[3] Shirgaonkar A A, Curet O M, Patankar N A et al.(2008). The hydrodynamics of ribbon-fin propulsion during impulsive motion. *J. Exp. Biol.*, 211, pp.3490-3503.
[4] Wu J Z, Ma H Y, Zhou M D(2006). *Vorticity and Vortex Dynamics*. Springer-Verlag., Berlin, Germany..
[5] Wu C J, Wang L, Wu J Z(2007). Suppression of the von Kármán vortex street behind a circular cylinder by a travelling wave generated by a flexible surface. *J. Fluid Mech.* 574 , pp. 365–391.
[6] Xin Z Q, Wu C J(2012). Numerical simulations and vorticity dynamics of self-propelled swimming of 3D bionic fish. *Sci. China-Phys. Mech. Astron.*,55(2) , pp.272-283.